

Imaging biomarkers of intrahepatic macrovascular tumour thrombus necrosis after combined therapies for advanced hepatocellular carcinoma: A downstaging indicator for radical surgery

Junning Cao

Chinese PLA General Hospital

Zhanbo Wang

Chinese PLA General Hospital

Bingyang Hu

Chinese PLA General Hospital

Wenwen Zhang

Chinese PLA General Hospital

Jun Han

Chinese PLA General Hospital

Tao Wan

Chinese PLA General Hospital

Shichun Lu (✉ lsc620213@aliyun.com)

Chinese PLA General Hospital <https://orcid.org/0000-0003-3278-0534>

Research

Keywords: Hepatocellular carcinoma, Tumour thrombus necrosis, Imaging biomarkers, Combined therapies, Downstaging

Posted Date: May 4th, 2021

DOI: <https://doi.org/10.21203/rs.3.rs-456053/v1>

License:   This work is licensed under a Creative Commons Attribution 4.0 International License.

[Read Full License](#)

Abstract

Background: As novel downstaging therapies are rising and the prevalence of advanced hepatocellular carcinoma (aHCC) with intrahepatic macrovascular tumour thrombus (IMTT) is high, accurate assessment of complete IMTT necrosis after these therapies could lead to an opportunity for subsequent radical surgery. Our preliminary study aimed to analyse the diagnostic accuracy of imaging biomarkers for complete IMTT necrosis after combined therapies for patients with aHCC.

Methods: Consecutive patients who were diagnosed with aHCC combined with IMTT at our single institute were treated with combined therapies (immune checkpoint inhibitors, tyrosine kinase inhibitors, or transarterial chemoembolization) and underwent radical surgery. Before and after combined therapies, contrast-enhanced or diffusion-weighted imaging was performed to assess complete IMTT necrosis. Image qualitative biomarkers, including disappearance of arterial enhancement and no diffusion restriction, were analysed. The percentage of IMTT enhancement (IMTTE%) and apparent diffusion coefficient (ADC) values were calculated. Receiver operating characteristic analysis was performed for IMTTE% and ADC values. Complete IMTT necrosis was confirmed by pathologic analysis. Differences were statistically significant when $P < 0.05$.

Results: There were 27 consecutive patients received combined therapies and underwent surgery. Eighteen patients with images from 36 examinations were included. Disappearance of arterial enhancement and no diffusion restriction yielded 88.9%/77.8% sensitivity, 83.3%/80.0% specificity, an 84.2%/82.4% positive predictive value, an 88.2%/75.0% negative predictive value, and 86.1%/78.8% diagnostic accuracy for diagnosing complete IMTT necrosis. The area under curve (AUC) of the IMTTE% values for the diagnosis of viable IMTT was 0.94, with an optimal cut-off value of 145.5% resulting in a sensitivity/specificity of 88.9%/88.9%. The AUC of ADC values for the diagnosis of complete IMTT necrosis was 0.79, with an optimal cut-off value of $1.3 \times 10^{-3} \text{ mm}^2/\text{s}$ resulting in a sensitivity/specificity of 88.9%/80.0%.

Conclusions: Contrast-enhanced and diffusion-weighted imaging biomarkers show good diagnostic performance in the differentiation of complete IMTT necrosis after combined therapies for patients with aHCC.

1. Background

Hepatocellular carcinoma (HCC) is a highly common cancer, accounting for approximately 90% of liver cancers^[1]. Radical hepatic resection or liver transplantation, by which long-term survival benefits can be achieved, is only recommended as the treatment of choice in patients with early-stage HCC (Barcelona Clinic Liver Cancer stage 0 or A)^[2]. It has been reported that 23.0-53.6% of HCC is diagnosed at the advanced stage with intrahepatic macrovascular tumour thrombus (IMTT), which has a poor overall survival (OS) of 6.9-15.6 months^[3-6]. In recent years, a variety of novel downstaging therapies, including hepatic arterial infusion chemotherapy, radioembolization, tyrosine kinase inhibitors (TKIs), and immune

checkpoint inhibitors (ICIs), have been applied for advanced HCC (aHCC), after which salvage surgery or transplantation could be performed^[7-10].

Complete IMTT necrosis is defined as the disappearance of arterial enhancement according to the modified Response Evaluation Criteria in Solid Tumours (mRECIST)^[11], which indicate that a successful downstaging for aHCC could be achieved more rapidly and often than complete regression of IMTT after treatment. Because the subsequent optimal surgery window is precious, it is crucial to assess complete IMTT necrosis accurately by radiologic imaging^[12].

As novel downstaging therapies are rising and there is a high prevalence of aHCC, accurate assessment of downstaging could lead to an opportunity for subsequent radical surgery and long-term survival benefits. Our preliminary study aimed to analyse the diagnostic accuracy of contrast-enhanced and diffusion-weighted imaging (DWI) biomarkers for complete IMTT necrosis after combined therapies.

2. Methods

2.1. Study design

From January 2019 to January 2021, consecutive patients who were diagnosed with aHCC at our single institute were treated with combined therapies [ICIs, TKIs, or transarterial chemoembolization (TACE)] and subsequent radical surgery.

2.2 Study population

The inclusion criteria included HCC diagnosed according to the criteria of the American Association for the Study of Liver Diseases^[13] and a diagnosis of IMTT by contrast-enhanced computed tomography (ceCT) or contrast-enhanced magnetic resonance imaging (ceMRI) according to the criteria described by Sherman CB^[14]. The exclusion criterion was incomplete IMTT necrosis after the combined therapy.

2.3. Standard medical procedures

Patients received downstaging therapies with one treatment of TACE and ICIs intravenously on day 1 of a 21-day cycle (one dose of pembrolizumab 200 mg, toripalimab 240 mg, sintilimab 200 mg or camrelizumab 200 mg) combined with TKIs orally daily [either lenvatinib (body weight \geq 60 kg, 12 mg; < 60 kg, 8 mg), sorafenib 0.4 g or apatinib 850 mg]. After each three cycles of therapy, ceMRI was performed to evaluate the response by assessing tumour size and viability. When the images showed complete IMTT necrosis or stable findings compared to the last image without complete IMTT necrosis, hepatic resection or liver transplantation was performed.

2.4. Imaging techniques

ceMRI was performed with a 1.5-T MR unit (uMR 560, United Imaging Healthcare, Shanghai, China) using contrast agents with gadopentetate dimeglumine. The axial diffusion-weighted sequence was performed

with b values of 50 and 800 sec/mm². The apparent diffusion coefficient (ADC) map was then generated on the imager console from the above two diffusion-weighted sequences. Axial T1-weighted examination was used to obtain unenhanced images and contrast-enhanced images. The contrast-enhanced image of the arterial phase was obtained at 18-20 s after contrast agent administration. ceCT was performed with a 64-detector CT (CT750 HD, GE Healthcare, Milwaukee, US) using contrast agents with iopromide. The axial examination included unenhanced images and contrast-enhanced images. Contrast-enhanced images of the arterial phase were obtained 20-30 s after contrast agent administration.

2.5. Image analysis

MR and CT images were evaluated with a picture archiving and communication system (Medcare, Medicon Digitalengineering, Qingdao, China) by two experienced liver surgeons (J.C. and S.L.) with six and 30 years of experience in liver imaging. All images showing the IMTT were selected as a reference for qualitative analysis, and the image showing the maximal diameter of the IMTT was selected as a reference for quantitative analysis. Polygonal regions of interest, which included at least 90% of the area of the IMTT, were drawn directly on the unenhanced images, contrast-enhanced images, and ADC images to obtain the quantitative values.

2.6. Image qualitative analysis

One of the imaging biomarkers indicating complete IMTT necrosis after combined therapy was defined as the disappearance of arterial enhancement relative to the surrounding liver parenchyma, according to mRECIST^[11]. The other biomarker was defined as no diffusion restriction indicated by the absence of hyperintense on diffusion-weighted images (b value of 800 sec/mm²), or hyperintense on diffusion-weighted images combined with absence of hypointense on ADC images.

2.7. Image quantitative analysis

The percentage of IMTT enhancement (IMTTE%) was calculated with signal intensity (SI) on the corresponding contrast-enhanced image (SI_{CE}) and the corresponding unenhanced image (SI_{UE}). IMTTE% was calculated by the following equation: $IMTTE\% = SI_{CE}/SI_{UE} \times 100\%$. The ADC value of IMTT was obtained from the corresponding ADC image.

2.8. Gold standard interpretation

IMTT was considered viable before the combined therapy. Complete IMTT necrosis after the combined therapy, which was indicated by the absence of any viable tumour cells, was confirmed by one pathologist (Z.W., with nine years of experience in liver disease) with a complete specimen slicing protocol. The pathologist was blind to the image analysis results.

2.9. Statistical analysis

SPSS 21.0 (IBM, NY, US) was used for statistical analysis. Descriptive statistics were reported as absolute numbers for categorical variables and as the mean (range) for continuous variables. Sensitivity, specificity, positive predictive value, negative predictive value, and diagnostic accuracy were calculated using standard statistical formulae. Differences between complete IMTT necrosis and viable IMTT were assessed using Mann-Whitney tests for continuous variables. Receiver operating characteristic (ROC) analysis was performed for IMTTE% values and ADC values. Differences were statistically significant when $P < 0.05$.

3. Results

There were 27 consecutive patients received combined therapies and underwent surgery. Complete IMTT necrosis after combined therapies was pathologically confirmed in 18 patients with HCC, including 15 males (83.3%) and 3 females (16.7%) with an average age of 54.5 ± 7.9 (38.0-68.0) years and an average BMI of 24.5 ± 2.2 (19.8-27.4) kg/m^2 . Patients received radical surgery after an average of 5.1 ± 1.6 (3.0-10.0) cycles of combined therapies. The combination regimens included pembrolizumab combined with lenvatinib (5/18), sintilimab combined with lenvatinib (5/18), sintilimab combined with lenvatinib and TACE (3/18), toripalimab combined with lenvatinib (2/18), pembrolizumab combined with lenvatinib and TACE (1/18), camrelizumab combined with sorafenib (1/18), and toripalimab combined with apatinib (1/18). Before the combined therapy, two patients underwent ceCT, and 16 patients underwent ceMRI, which included the diffusion-weighted sequence in 15 patients. All 18 patients underwent ceMRI (all including the diffusion-weighted sequence) before the subsequent surgery (Figure 1).

Diagnostic results obtained from the qualitative features observed in the images of complete IMTT necrosis are shown in Table 1 and Figure 2. The differences in IMTTE% values [122.2 ± 24.7 (95.0-199.0) vs. 206.1 ± 73.0 (136.0-387.0) %, $P < 0.001$] and ADC values [1.6 ± 0.4 (0.8-2.2) vs. 1.2 ± 0.3 (0.8-1.9) $\times 10^{-3} \text{ mm}^2/\text{s}$, $P = 0.004$] were statistically significant between complete IMTT necrosis and viable IMTT.

The ROC analysis showed that the area under curve (AUC) of IMTTE% values for the diagnosis of viable IMTT was 0.94 ($P < 0.001$), with an optimal cut-off value of 145.5% resulting in a sensitivity/specificity of 88.9%/88.9% (Figure 3). The AUC of ADC values for the diagnosis of complete IMTT necrosis was 0.79 ($P = 0.004$), with an optimal cut-off value of $1.3 \times 10^{-3} \text{ mm}^2/\text{s}$ resulting in a sensitivity/specificity of 88.9%/80.0% (Figure 4).

4. Discussion

To the best of our knowledge, previous studies have mainly focused on the differentiation of malignant thrombus from bland thrombus in patients with HCC^[14, 15], and the assessment of complete IMTT necrosis after locoregional or systemic therapies has not been reported. As the benefits achieved from the promising combination of ICIs and TKIs are increasing^[16, 17], downstaging therapies for aHCC will become frequent. It is not feasible to perform biopsies of IMTT because of the complicated puncture access and the potential risk for bleeding. Although the gold standard diagnosis is pathologic analysis,

imaging analysis plays a pivotal role in clinical practice. Our preliminary study shows that complete IMTT necrosis as an indicator of the efficacy of downstaging therapies could be accurately assessed with contrast-enhanced and DWI features, which is crucial for liver surgeons to be able to recommend subsequent radical surgery.

Similar to the tumour lesions of HCC, arterial enhancement was considered a major imaging feature for IMTT^[14, 18]. ceMRI for detecting arterial enhancement has been demonstrated to provide good diagnostic performance in the detection of IMTT, with a diagnostic accuracy of 92.0-95.0% and a sensitivity of 79.0-95.0%^[15]. When tumours become completely necrotic, the intratumoural arterial blood supply will be destroyed, leading to the disappearance of intratumoural arterial enhancement. Arizumi T^[19] reported that patients with aHCC who showed complete disappearance of tumour enhancement after TKIs therapy had better OS rates than patients with no enhancement change. A sensitivity of 88.9% in this study demonstrates that the disappearance of arterial enhancement after combined therapies can be a reliable imaging biomarker that indicates complete IMTT necrosis, and the decrease in the mean IMTTE% value from $206.1 \pm 73.0\%$ to $122.2 \pm 24.7\%$ ($P < 0.001$) also indicates that necrosis can be measured as a quantitative reference.

Diffusion restriction as an ancillary imaging feature has been widely applied for the diagnosis of HCC lesions and IMTT^[18, 20]. DWI that does not require contrast agent administration could be feasible instead of contrast-enhanced imaging, especially for patients with renal insufficiency or other contraindications to contrast agent. Diffusion of water molecules is restricted in viable IMTT, yielding lower ADC values, whereas necrosis leads to unrestricted diffusion^[20, 21]. Lu TL reported that^[22] pretreatment ADC values of HCC lesions increased from $1.2 \pm 0.3 \times 10^{-3} \text{ mm}^2/\text{s}$ to $1.5 \pm 0.3 \times 10^{-3} \text{ mm}^2/\text{s}$ at six months after radiofrequency ablation. Our study also showed the same increasing trend in the mean ADC value of complete IMTT necrosis (1.6 ± 0.4 vs. $1.2 \pm 0.3 \times 10^{-3} \text{ mm}^2/\text{s}$, $P = 0.004$). A specificity of 80.0% in our study suggested that diffusion restriction after the combined therapy could be an ancillary imaging biomarker for the differentiation of viable IMTT from complete necrosis.

Sandrasegaran K^[23] reported that arterial enhancement yielded an AUC of 0.73 for the diagnosis of malignant portal vein thrombosis on ROC analysis, and ADC measurements yielded an AUC of 0.66. The ROC analysis in our study showed higher AUCs for both IMTTE% values and ADC values in the differentiation of complete necrosis from viable IMTT (0.94 and 0.79, respectively), which indicated that the imaging features were functional not only for diagnosis but also for therapeutic response assessment for IMTT.

The main limitation of this study was the relatively small number of patients. Another limitation was that not all the patients underwent ceMRI and diffusion-weighted sequence before the combined therapy. Therefore, selective bias could not be fully avoided. Further studies including more patients are necessary to validate the reported imaging biomarkers as indicators of complete IMTT necrosis.

5. Conclusion

Our preliminary study shows good diagnostic performance of contrast-enhanced and diffusion-weighted imaging biomarkers for the differentiation of complete IMTT necrosis after combined therapies for patients with HCC. Accurate assessment of complete IMTT necrosis will contribute to determining the optimal timing of subsequent radical surgery and improving long-term survival benefits.

Abbreviations

HCC: Hepatocellular carcinoma; IMTT: Intrahepatic macrovascular tumour thrombus; OS: Overall survival; TKIs: Tyrosine kinase inhibitors; ICIs: Immune checkpoint inhibitors; aHCC: Advanced hepatocellular carcinoma; mRECIST: Modified Response Evaluation Criteria in Solid Tumours; DWI: Diffusion-weighted imaging; TACE: Transarterial chemoembolization; ceCT: Contrast-enhanced computed tomography; ceMRI: Contrast-enhanced magnetic resonance imaging; ADC: Apparent diffusion coefficient; IMTTE%: Percentage of IMTT enhancement; SI: Signal intensity; SICE: SI on the corresponding contrast-enhanced image; SIUE: SI on the corresponding unenhanced image; ROC: Receiver operating characteristic; AUC: Area under curve

Declarations

Ethics approval and consent to participate

This study was approved by the Ethics Committee of Chinese PLA General Hospital (S2018-111-01). Written informed consent was obtained from each participant.

Consent for publication

Written informed consent for publication was obtained from each participant.

Availability of data and materials

The datasets used or analysed during the current study are available from the corresponding author on reasonable request.

Competing interests

The authors declare no conflicts of interest in this work.

Funding

This study was supported by the National Natural Science Foundation of China (No.81670590).

Authors' contributions

Dr. Junning Cao, designer of this work, made substantial contributions to conception, design, collection and interpretation of the clinical data, image analysis, drafting the article and revising it critically. Dr. Shichun Lu, designer and principal investigator of this work, made substantial contributions to conception, design, surgical procedure, image analysis, interpretation of the clinical data, and gave final approval of the version to be published. Dr. Zhanbo Wang, contributed to the proposal and design of this work, pathological analysis of patient series, data collection, drafting and revision of the manuscript and figures in his perspective. Dr. Bingyang Hu, Wenwen Zhang, Jun Han, Tao Wan contributed to the proposal and design of this work, data collection, patient follow-ups, drafting and revision of the manuscript.

Acknowledgements

We are grateful to Dr. Mengqiu Cui for providing general support for this study.

References

- [1] Llovet JM, Zucman-Rossi J, Pikarsky E, et al. Hepatocellular carcinoma. *Nat Rev Dis Primers*. 2016. 2: 16018.
- [2] EASL Clinical Practice Guidelines: Management of hepatocellular carcinoma. *J Hepatol*. 2018. 69(1): 182-236.
- [3] Xiang X, Zhong JH, Wang YY, et al. Distribution of tumor stage and initial treatment modality in patients with primary hepatocellular carcinoma. *Clin Transl Oncol*. 2017. 19(7): 891-897.
- [4] Giannini EG, Farinati F, Ciccarese F, et al. Prognosis of untreated hepatocellular carcinoma. *Hepatology*. 2015. 61(1): 184-190.
- [5] Cabibbo G, Maida M, Genco C, et al. Natural history of untreatable hepatocellular carcinoma: A retrospective cohort study. *World J Hepatol*. 2012. 4(9): 256-261.
- [6] Liu BJ, Gao S, Zhu X, et al. Sorafenib combined with embolization plus hepatic arterial infusion chemotherapy for inoperable hepatocellular carcinoma. *World J Gastrointest Oncol*. 2020. 12(6): 663-676.
- [7] Levi SGB, Ettorre GM, Colasanti M, et al. Hepatocellular carcinoma with macrovascular invasion treated with yttrium-90 radioembolization prior to transplantation. *Hepatobiliary Surg Nutr*. 2017. 6(1): 44-48.
- [8] Schwacha-Eipper B, Minciuna I, Banz V, Dufour JF. Immunotherapy as a downstaging therapy for liver transplantation. *Hepatology*. 2020. 72(4): 1488-1490.
- [9] Goto Y, Hisaka T, Sakai H, et al. Salvage Surgery for Initially Unresectable Locally Advanced Hepatocellular Carcinoma Downstaged by Hepatic Arterial Infusion Chemotherapy. *Anticancer Res*. 2020.

40(8): 4773-4777.

- [10] Kermiche-Rahali S, Di FA, Drieux F, et al. Complete pathological regression of hepatocellular carcinoma with portal vein thrombosis treated with sorafenib. *World J Surg Oncol*. 2013. 11(1): 171.
- [11] Lencioni R, Llovet JM. Modified RECIST (mRECIST) assessment for hepatocellular carcinoma. *Semin Liver Dis*. 2010. 30(1): 52-60.
- [12] Forner A, Reig M, Bruix J. Hepatocellular carcinoma. *Lancet*. 2018. 391(10127): 1301-1314.
- [13] Heimbach JK, Kulik LM, Finn RS, et al. AASLD guidelines for the treatment of hepatocellular carcinoma. *Hepatology*. 2018. 67(1): 358-380.
- [14] Sherman CB, Behr S, Dodge JL, et al. Distinguishing Tumor From Bland Portal Vein Thrombus in Liver Transplant Candidates With Hepatocellular Carcinoma: the A-VENA Criteria. *Liver Transpl*. 2019. 25(2): 207-216.
- [15] Kim JH, Lee JM, Yoon JH, et al. Portal Vein Thrombosis in Patients with Hepatocellular Carcinoma: Diagnostic Accuracy of Gadoteric Acid-enhanced MR Imaging. *Radiology*. 2016. 279(3): 773-783.
- [16] Finn RS, Ikeda M, Zhu AX, et al. Phase Ib Study of Lenvatinib Plus Pembrolizumab in Patients With Unresectable Hepatocellular Carcinoma. *J Clin Oncol*. 2020. 38(26): 2960-2970.
- [17] Yau T, Hsu C, Kim TY, et al. Nivolumab in advanced hepatocellular carcinoma: Sorafenib-experienced Asian cohort analysis. *J Hepatol*. 2019. 71(3): 543-552.
- [18] Chernyak V, Fowler KJ, Kamaya A, et al. Liver Imaging Reporting and Data System (LI-RADS) Version 2018: Imaging of Hepatocellular Carcinoma in At-Risk Patients. *Radiology*. 2018. 289(3): 816-830.
- [19] Arizumi T, Ueshima K, Chishina H, et al. Decreased blood flow after sorafenib administration is an imaging biomarker to predict overall survival in patients with advanced hepatocellular carcinoma. *Dig Dis*. 2014. 32(6): 733-739.
- [20] Catalano OA, Choy G, Zhu A, et al. Differentiation of malignant thrombus from bland thrombus of the portal vein in patients with hepatocellular carcinoma: application of diffusion-weighted MR imaging. *Radiology*. 2010. 254(1): 154-162.
- [21] Granata V, Fusco R, Amato DM, et al. Beyond the vascular profile: conventional DWI, IVIM and kurtosis in the assessment of hepatocellular carcinoma. *Eur Rev Med Pharmacol Sci*. 2020. 24(13): 7284-7293.

[22] Lu TL, Becce F, Bize P, et al. Assessment of liver tumor response by high-field (3 T) MRI after radiofrequency ablation: short- and mid-term evolution of diffusion parameters within the ablation zone. *Eur J Radiol.* 2012. 81(9): e944-e950.

[23] Sandrasegaran K, Tahir B, Nutakki K, et al. Usefulness of conventional MRI sequences and diffusion-weighted imaging in differentiating malignant from benign portal vein thrombus in cirrhotic patients. *AJR Am J Roentgenol.* 2013. 201(6): 1211-1219.

Table

Table 1. Image qualitative diagnosis of tumour thrombus

		Complete necrosis (n)	Viable (n)	Sensitivity (%)	Specificity (%)	PPV ^a (%)	NPV ^b (%)	Accuracy ^c (%)
Arterial enhancement	No	16	3	88.9	83.3	84.2	88.2	86.1
	Yes	2	15					
Diffusion restriction	No	14	3	77.8	80.0	82.4	75.0	78.8
	Yes	4	12					

^a Positive predictive value; ^b Negative predictive value; ^c Diagnostic accuracy.

Figures

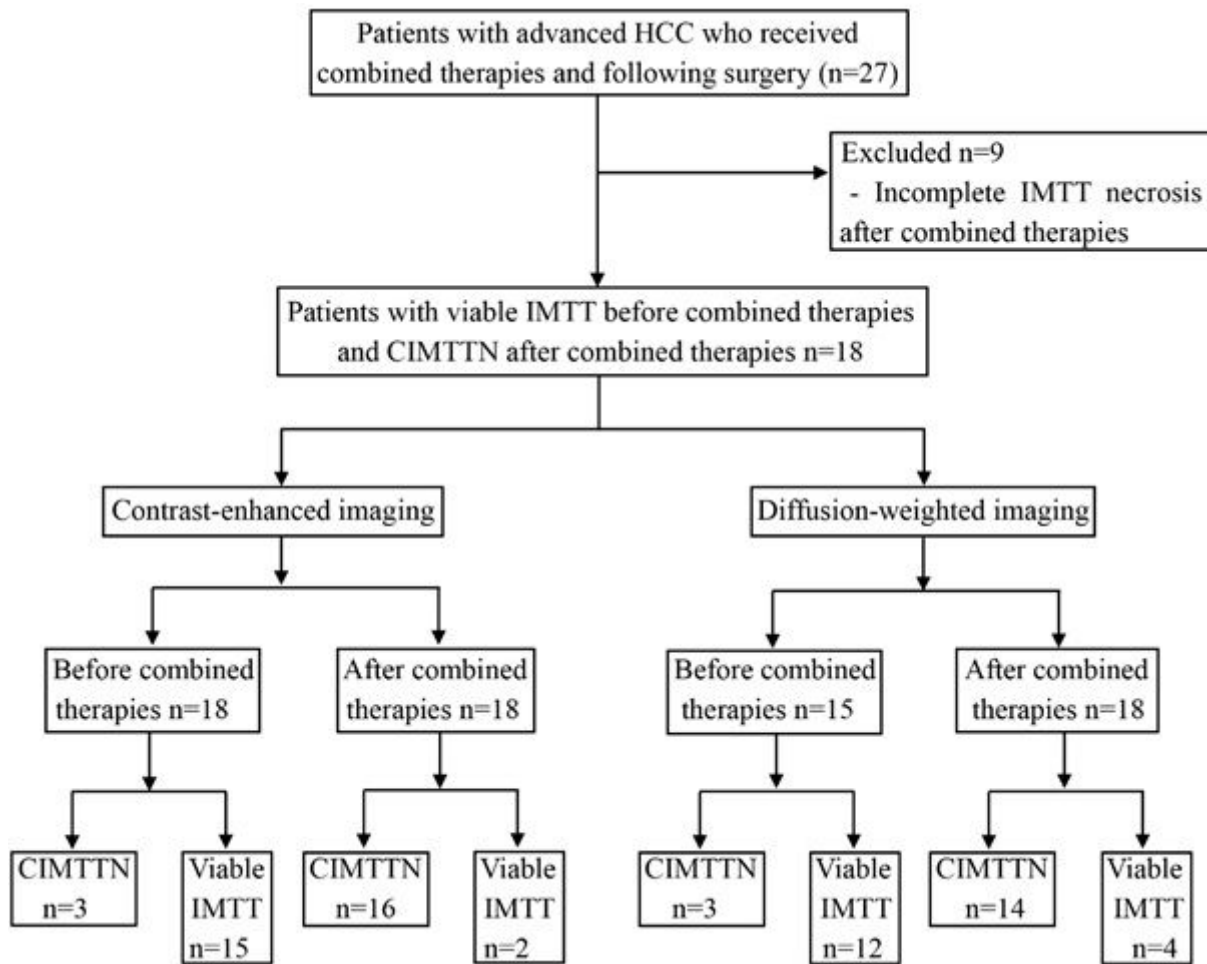


Figure 1

Flow diagram of study patients.

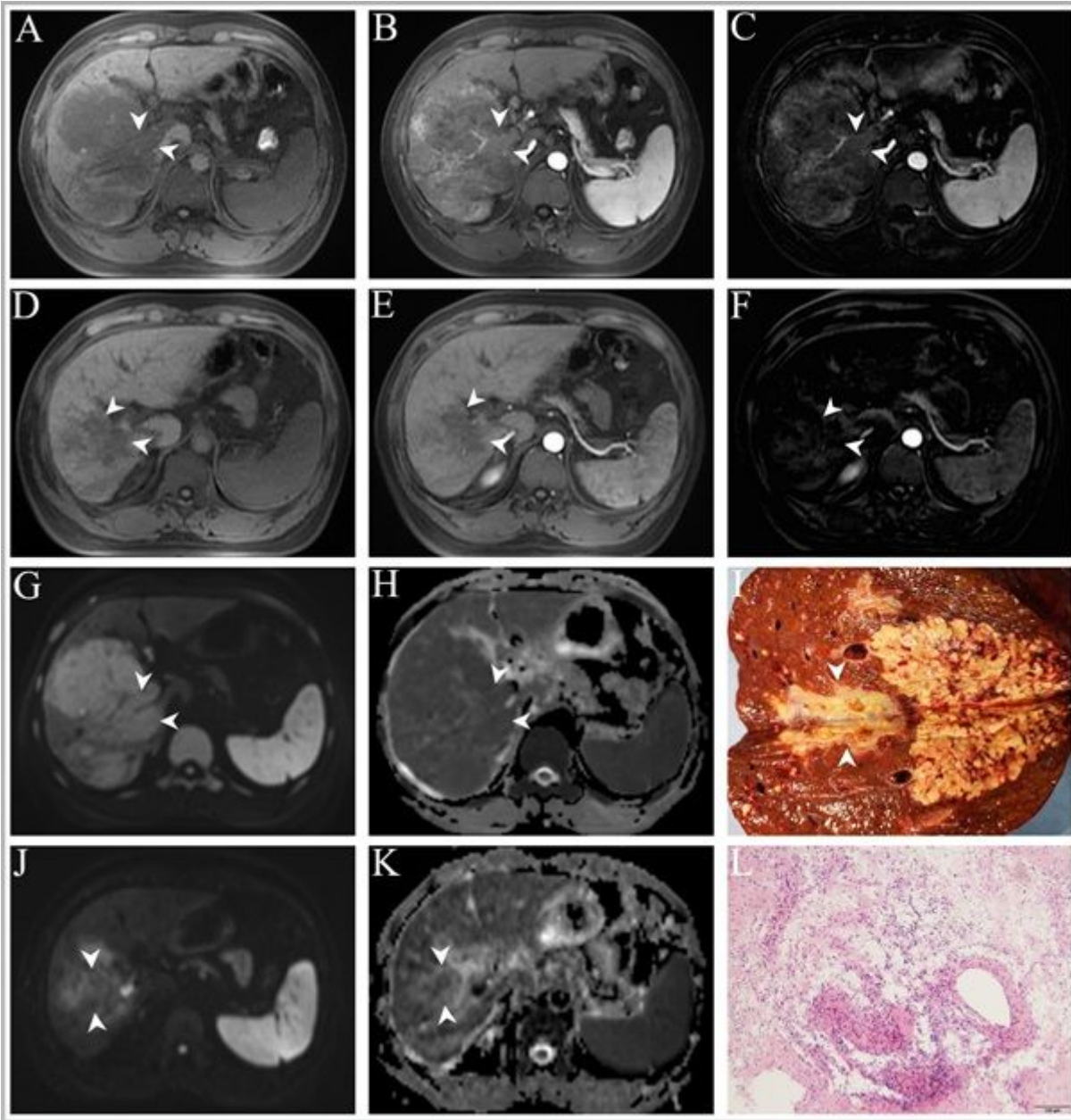


Figure 2

Radiologic, specimen and pathologic images of one patient with complete tumour thrombus necrosis after combined therapy. The tumour thrombus is indicated with white arrowheads in each image. Contrast-enhanced axial MR images before combined therapy: The viable tumour thrombus was hypointense on the precontrast T1 image (A), hyperintense on the postcontrast arterial phase image (B), hyperintense on the subtracted arterial phase image (C), hyperintense on the diffusion-weighted image obtained with a b value of 800 sec/mm² (G), and mildly hypointense on the apparent diffusion coefficient image (H). Contrast-enhanced axial MR images after combined therapy: Complete tumour thrombus necrosis was hypointense on precontrast T1 images (D), hypointense on the postcontrast arterial phase image (E), hypointense on the subtracted arterial phase image (F), hyperintense on the diffusion-weighted image obtained with a b value of 800 sec/mm² (J), and hyperintense on the apparent

diffusion coefficient image (K). Complete necrosis of the tumour thrombus was seen in specimen (I) and confirmed by pathology (L).

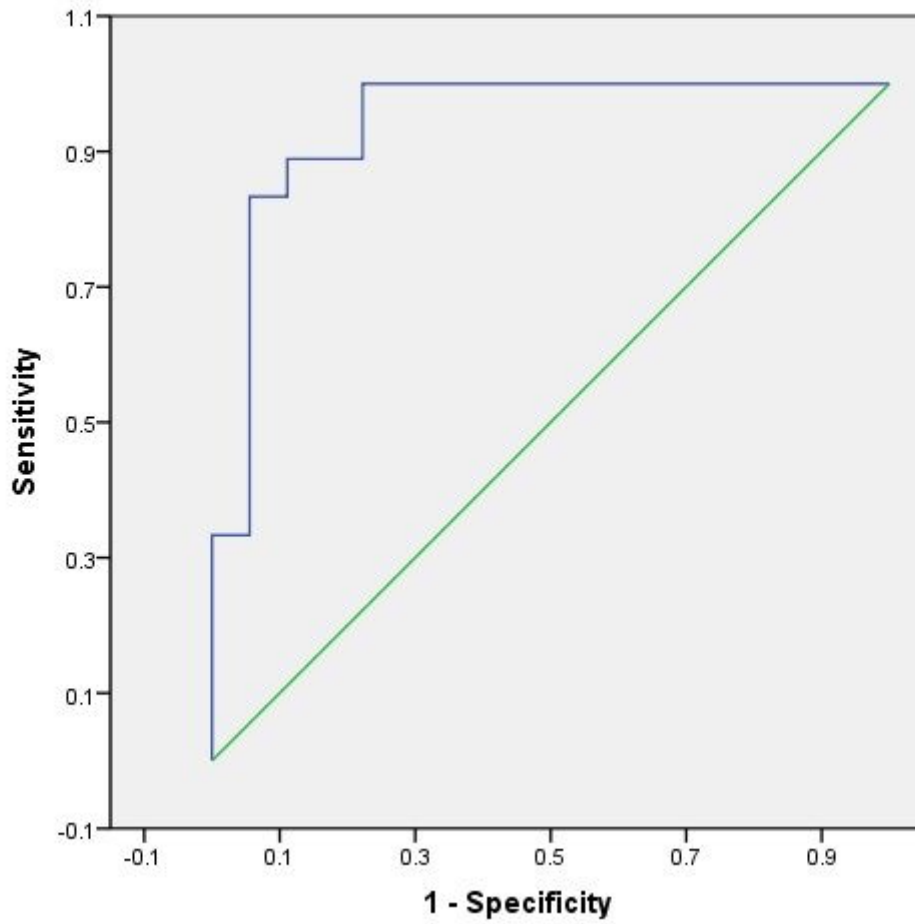


Figure 3

Receiver operating characteristic curves of the percentage of enhancement in the diagnosis of viable tumour thrombus.

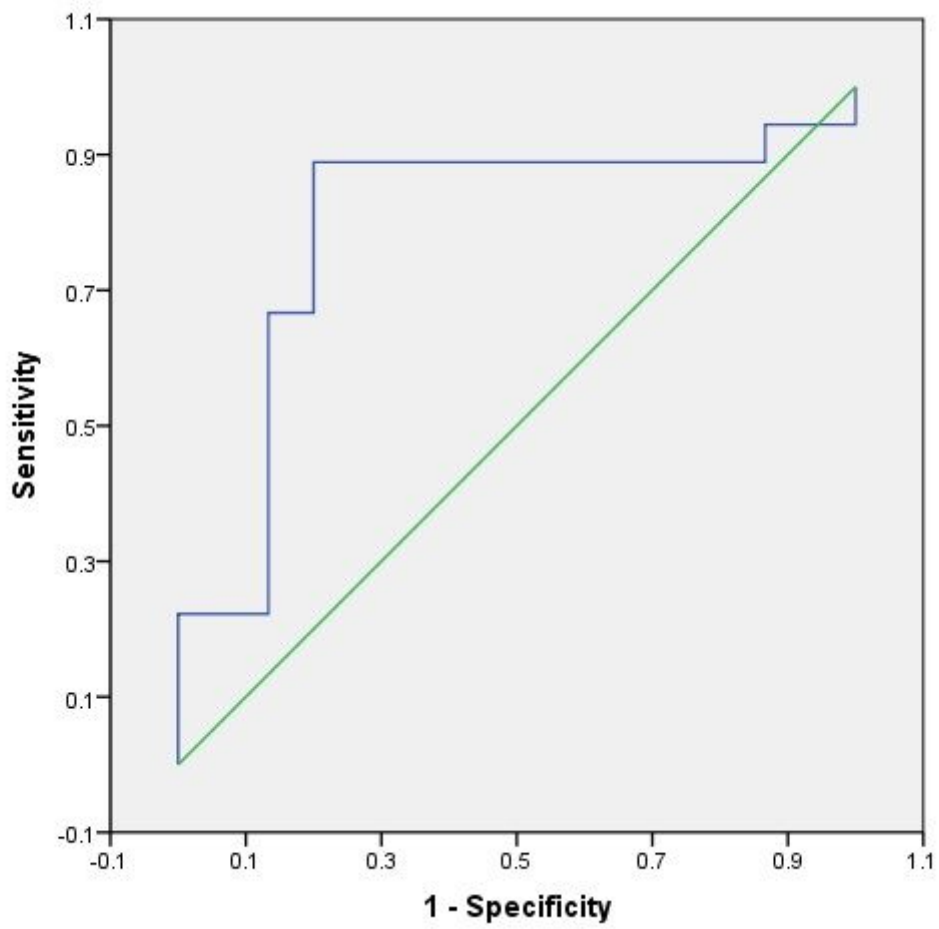


Figure 4

Receiver operating characteristic curves of the apparent diffusion coefficient values in the diagnosis of complete tumour thrombus necrosis.